

Magnetic-field-induced crystallographic texture enhancement in cold-deformed FePt nanostructured magnets

B. Z. Cui^(a) and K. Han

National High Magnetic Field Laboratory, Florida State University, Tallahassee, Florida 32310

D. S. Li and H. Garmestani

School of Materials Science and Engineering, Georgia Institute of Technology, Atlanta, Georgia 30332

J. P. Liu

Department of Physics, University of Texas at Arlington, Arlington, Texas 76019

N. M. Dempsey

Laboratoire Louis Néel, 25 avenue des Martyrs, BP 166, 38042 Grenoble, France

H. J. Schneider-Muntau

National High Magnetic Field Laboratory, Florida State University, Tallahassee, Florida 32310

(Received 16 December 2005; accepted 26 March 2006; published online 5 July 2006)

This paper reports a unique approach to the fabrication of magnetically anisotropic nanostructured FePt magnets: cyclic sheath cold rolling and subsequent magnetic annealing. High magnetic fields enhance both crystallographic texture and magnetic properties of cold-deformed FePt nanostructured magnets. Magnetic annealing increases (001) out-of-plane texture of the FePt hard phase by 50% and introduces magnetic anisotropy in the annealed samples. It is suggested that pret textured Fe and Pt nanocrystals provide favorable nucleation sites for magnetic-field-induced nucleation and growth of textured FePt grains. It is argued that the enhancement of texture of the FePt hard phase and promotion of the solid-state phase transformation by magnetic annealing are the reasons for improvement of the magnetic properties. © 2006 American Institute of Physics.

[DOI: [10.1063/1.2206410](https://doi.org/10.1063/1.2206410)]

I. INTRODUCTION

Ordered FePt with the face-centered tetragonal (fct) $L1_0$ structure exhibits excellent intrinsic magnetic properties and is therefore a suitable candidate for permanent magnet applications and ultrahigh-density magnetic recording media.¹ The theoretical energy product value is expected for homogenized and textured nanostructured FePt permanent magnets.^{2,3} In particular, the alignment of the hard nanograins to achieve strong c -axis texture and magnetic anisotropy is essential in attainment of record high $(BH)_{\max}$ in either nanocomposites or single-phase nanostructured magnets.²⁻⁴ In this paper, we report a unique approach to obtain anisotropic nanostructured FePt magnets with crystallographic texture of the hard phase: severe plastic deformation (SPD, cyclic cold rolling in this paper) and subsequent magnetic annealing.⁵ The SPD produced nanostructured Fe-Pt multilayers are highly textured and uniform, and subsequent magnetic annealing promoted the fct FePt phase formation in certain crystal orientations so that the magnetic properties are improved.

II. EXPERIMENTAL PROCEDURE

For the preparation of equiatomic FePt, the cyclic sheath cold rolling of a composite stack of 12 bilayers of Fe and Pt foils [Fe(75 μm)/Pt(100 μm)]₁₂ was used to create a nano-

laminate Fe/Pt foil. In a given rolling cycle of about 100 passes, the total thickness was reduced by a factor of 10. The rolling was undertaken without intermediate heat treatment. The sample was submitted to four such rolling cycles (cumulative reduction factor $\approx 10^4$). The details about the preparation of the as-rolled Fe/Pt nanolaminate foil are given in the Refs. 6 and 7. The multilayered foils were about $20 \times 12 \times 0.1 \text{ mm}^3$ in size. Samples of $4 \times 3 \times 0.1 \text{ mm}^3$ were cut from the central part of the foils. Three categories of samples were annealed at 455 °C for 120 min. NF sample was annealed without a magnetic field, IPF sample was annealed with a 19 T in-plane field, i.e., the field was parallel to the rolling direction (RD), and OPF sample was annealed with a 19 T out-of-plane field, i.e., the field was parallel to the normal direction (ND) of the foil plane. The 19 T field was applied when the sample temperature was raised up to 200 °C. The high field was reduced to zero when the samples were cooled down below 200 °C after annealing.

Phase components of the samples were identified by x-ray diffraction (XRD) using Cu $K\alpha$ radiation. Texture of the hard FePt phase was measured using a Philips X'Pert PW3040 MRD x-ray diffractometer, equipped with a pole figure goniometer, operating at 40 kV and 45 mA and employing Ni filtered Cu $K\alpha$ radiation. Incomplete pole figures of (110), (200), (002), (201), and (202) for the fct FePt phase were obtained. After the correction of the geometric defocusing and background x-ray intensity, a spherical harmonics algorithm implemented in popLA was used to calculate the crystal orientation distribution from which the recalculated

^(a)Author to whom correspondence should be addressed; FAX: 850-644-0867; electronic mail: cuiبز@yahoo.com

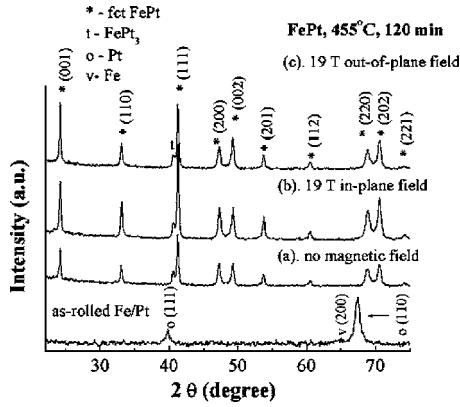


FIG. 1. XRD patterns of the FePt foils annealed at 455 °C for 120 min (a) without a field, (b) with a 19 T in-plane field, (c) with a 19 T out-of-plane field. XRD pattern of the as-rolled Fe/Pt is also given in Fig. 1.

pole figures were constructed.⁸ The error in normalized intensities of the texture components is smaller than 0.05 times random. The magnetic properties at 5 K were measured using a Quantum Design superconducting quantum interference device (SQUID) magnetometer in fields up to 7 T.

III. RESULTS AND DISCUSSIONS

Scanning electron microscopy images of the as-rolled Fe/Pt multilayered foil showed that the individual layer thickness after four deformation cycles was of the order of several tens of nanometers, in agreement with the bulk reduction factor.^{6,7,9} XRD investigations demonstrated that the Fe and Pt nanocrystals have (001) and (011) out-of-plane textures in the as-rolled foil, respectively.^{6,7} Therefore, the orientation relationship is (001)_{Fe}|| (011)_{Pt},⁹ which is different from the orientation relationship observed in the Fe/Pt multilayers prepared by sputter deposition.¹⁰

Annealing the Fe/Pt multilayered foils at 455 °C for 120 min leads to the formation of nanostructured fct FePt hard phase, accompanied by a small amount of the antiferromagnetic FePt₃ phase (see Fig. 1). The average grain size of fct FePt phase is 20 nm in this work, calculated from the (002) diffraction peak using the Scherrer formula. Previous studies indicate that the grain sizes vary from tens of nanometers to a few hundreds of nanometers.^{6,7} It is noted that intensities of the (001) and (002) diffraction peaks of the FePt hard phase increase after magnetic annealing in a 19 T out-of-plane field. This is manifested by comparison of the (200) diffraction peak with the (002) one. The I_{002}/I_{200} values of the FePt hard phase are 1.0, 0.98, and 1.56 for the NF, IPF, and OPF samples, respectively, where I_{002} and I_{200} are the integrated intensities of (002) and (200) diffraction

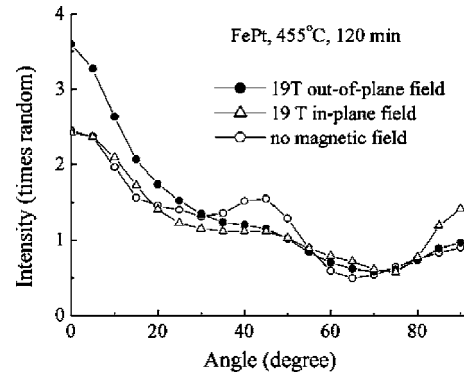


FIG. 3. Distribution of *c* axes of the FePt crystals tilted away from the normal direction of the foil plane for the three samples of Fig. 2.

peaks. The annealing with a 19 T out-of-plane field (OPF sample) results in the greatest I_{002}/I_{200} among all the samples. This indicates that there is an obvious enhancement of the (001) out-of-plane texture of the FePt hard phase in the OPF sample, whereas the I_{002}/I_{200} values for the NF and IPF samples are only marginally different, within the error bar of 5%. It should be noted that the I_{002}/I_{200} value for randomly oriented fct FePt powder is only 0.52, obtained from JCPDS 43-1359.¹¹ This suggests that there is a (001) out-of-plane texture of the FePt hard phase in all the annealed samples. The texture of the FePt hard phase was further evaluated by pole figures. Figure 2 shows recalculated (001) pole figures of the FePt hard phase of the NF, IPF, and OPF samples. Figure 3 shows the quantitative distribution of *c* axes of the FePt crystals tilted away from the normal direction of the foil plane for the three samples of Fig. 2. It is obtained from the integration of the pole figures shown in Fig. 2 along the azimuthal direction. As shown in Figs. 2(a) and 3, in the NF sample (which was annealed without a field), the distribution intensity of crystal *c* axes parallel to the ND is 2.4 times random. This indicates that the NF sample has a preferential orientation of *c* axes (easy magnetization axis) of the FePt phase parallel to the ND, i.e., the FePt phase in this sample is (001) out-of-plane textured. This corresponds to an orientation relationship of (001)_{Fe}|| (001)_{FePt}|| (011)_{Pt}. The formation of this texture of the FePt phase is attributed to the cold-rolling-induced textures in both Fe and Pt phases. It can be deduced that the FePt nucleated to adapt the (001)_{Fe}|| (011)_{Pt} orientation relationship. The other important factor is the preferred nucleation sites. The formation of FePt (fct) in the as-rolled nanolaminate Fe/Pt foil should occur at interfaces of Fe and Pt at 455 °C. The pretextured Fe and Pt induces the fct FePt grains with preferred crystallographic orientation as a result

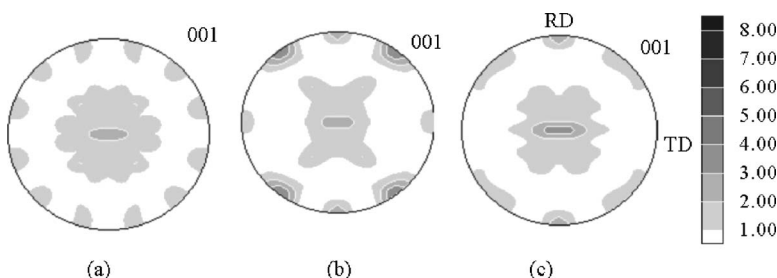


FIG. 2. (001) pole figures of the FePt hard phase in the FePt alloys annealed at 455 °C for 120 min (a) without a field, (b) with a 19 T in-plane field, and (c) with a 19 T out-of-plane field. Note: TD is the transverse direction, while the crosshair corresponds to the ND of the sample.

of defined habit plane for the nucleation and orientation relationship among Fe, Pt nanocrystals, and fct FePt phases. If the fct FePt phase nucleates on $(001)_{\text{Fe}}$ and $\langle 100 \rangle_{\text{FePt}}$ is parallel to $\langle 110 \rangle_{\text{Pt}}$, the lattice mismatch is 5%. All other orientation relationships introduce more misfits in the system. Similarly, when the fct FePt phase nucleates with $(001)_{\text{FePt}} \parallel (011)_{\text{Pt}}$ and $\langle 100 \rangle_{\text{FePt}} \parallel \langle 100 \rangle_{\text{Pt}}$, the misfit is merely 2%. Therefore, minimization of the misfit interface energy controls the nucleation and growth of fct FePt phase in the NF sample.

Magnetic annealing influences the distribution of the c axes of the FePt nanocrystals. As shown in Figs. 2 and 3, compared with the sample annealed without a field, the distribution intensity of c axes of the FePt crystals along the ND increases by 50% (from 2.4 to 3.6 times random) in the sample annealed with a 19 T out-of-plane field, which is still the strongest texture component. The value in the sample annealed with a 19 T in-plane field is the same as that of the sample annealed without a field. This indicates that the external field of 19 T is only strong enough to reorientate the grains to less than 90° . On the other hand, the distribution intensity of c axes of the FePt crystals in the foil plane increases from 0.97 to 1.4 times random in the IPF sample, as shown in Fig. 3. The intensity of texture component with c axes of the FePt crystals parallel to the RD increases from 0.2 to 2.7 times random, as shown in Fig. 2. Therefore, it can be seen that compared with the sample annealed without a field, there is a preferential orientation trend of c axes of the FePt nanocrystallites along the magnetic-field direction in the magnetically annealed samples.

The magnetic annealing temperature in this work (455°C) is lower than the Curie temperature of the FePt hard phase (477°C).¹² In the magnetic-field-assisted phase transformation, the driving force due to the magnetocrystalline anisotropy energy of ferromagnetic FePt phase could overcome the energy barriers associated with the shape anisotropy and the thermal disordering, if the applied magnetic field is high enough.¹³ In this case, the hard-phase-textured nanostructure with the easy axes parallel to the external field has lower free energy than a random structure, and therefore could be preferably formed. Therefore, the growth of textured FePt phase is attributed to both the texture inheritance from the pre-textured Fe and Pt nanocrystals that provides favorable nucleation sites and magnetic-field-induced texture.

The hysteresis curves of the annealed FePt samples measured with applied fields parallel and perpendicular to the foil plane are termed as in-plane (IP) and out-of-plane (OP) hysteresis curves in this paper, respectively. Figure 4 shows typical low field portions of half hysteresis loops of the NF and OPF samples. The magnetic results of all the samples are shown in Table I. Magnetically anisotropic behavior was clearly found in all the annealed samples, resulting from the textures of the FePt phase discussed above. Compared with the sample annealed without a field, magnetically annealed samples demonstrate an improvement in remanence J_r , and energy product $(BH)_{\text{max}}$. $(BH)_{\text{max}}$ was increased by 18%–19%. The highest $(BH)_{\text{max}}$ of 90.7 kJ/m^3 and J_r of 0.82 T from the OP hysteresis curves were obtained in the OPF

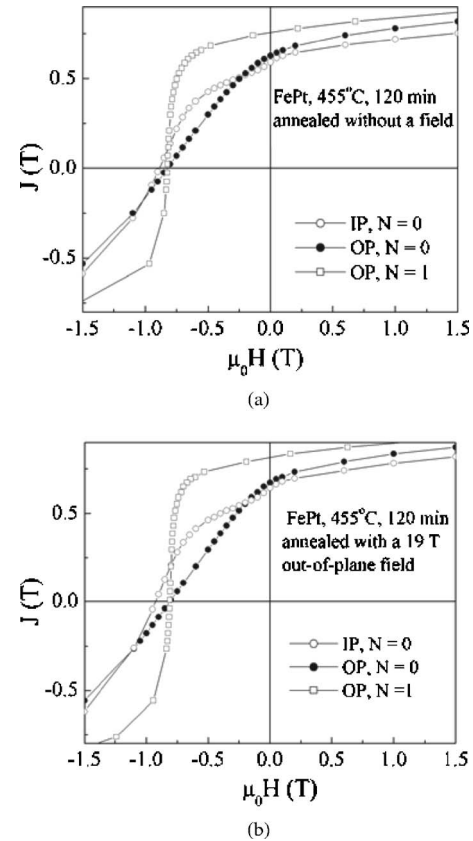


FIG. 4. Hysteresis loops of FePt samples annealed at 455°C for 120 min (a) without and (b) with a 19 T out-of-plane (N is the demagnetization factor).

sample, which has the strongest (001) out-of-plane texture. In the case of in-plane measurements, the IPF sample has the highest $(BH)_{\text{max}}$ and J_r because of its strongest (001) in-plane texture. In addition, the $(BH)_{\text{max}}$ and J_r from the OP hysteresis curves are higher than those from the IP ones because the (001) out-of-plane texture is dominant in all the samples, as shown in Figs. 2 and 3.

In our previous work, the as-rolled Fe/Pt nanolaminate foils were also annealed at temperatures ranging from 500 to 1010°C for 20–210 min with and without a 19 T field, which is above the Curie temperature of the FePt hard phase.¹⁴ Similar nanostructural, textural, and magnetic results were obtained for these FePt samples as those of the

TABLE I. Magnetic properties of the three samples of Fig. 2. Error bars for $\mu_0 H_c$, J_r , and $(BH)_{\text{max}}$ are 0.5%, 0.5%, and 1%, respectively. Note: N is the demagnetization factor.

Samples	From the IP hysteresis curves with $N=0$			From the OP hysteresis curves with $N=1$		
	$\mu_0 H_c$ (T)	$(BH)_{\text{max}}$ (kJ/m^3)	J_r (T)	$\mu_0 H_c$ (T)	$(BH)_{\text{max}}$ (kJ/m^3)	J_r (T)
NF (without a field)	0.89	52.5	0.59	0.82	76.5	0.76
IPF (19 T in-plane field)	0.9	61.9	0.65	0.87	81.2	0.79
OPF (19 T out-of-plane field)	0.93	58.7	0.64	0.81	90.7	0.82

samples annealed at 455 °C for 120 min in this paper.¹⁴ On the other hand, both high annealing temperature and long annealing time benefit completion of the diffusion of Fe and Pt atoms and the ordering phase transformation to completely form fct FePt, and further, decrease the relative volume fraction of FePt₃ phase in the annealed FePt sample. Especially, a single fct FePt phase was obtained in the FePt sample annealed at 1010 °C for 20 min.¹⁴ However, the grain growth of the fct phase and the decrease of the domain wall energy associated with pinning sites lead to a monotonous decrease of the coercivity and/or energy product of the FePt samples with increasing the annealing temperature or the annealing time.¹⁴

It should be noted that magnetic annealing does not only enhance the texture of the FePt hard phase but also accelerates the nucleation rate of ferromagnetic grains.¹⁵⁻¹⁷ The improvement in the magnetic properties is a comprehensive result of the magnetic-field-induced enhancement of crystallographic textures of the fct FePt phase and the promotion of the solid-state phase transformation through an increase of nucleation rate of the ordered FePt phase by magnetic annealing.¹⁵⁻¹⁷ On the other hand, compared with cyclic cold rolling, much stronger and different kinds of pretextures of Fe and Pt may be formed by other SPD methods, such as cyclic cold drawing, equal channel angular extrusion, high pressure torsion, etc.⁵ Further improvements of crystallographic textures and magnetic properties are expected by optimizing the SPD and magnetic annealing conditions. Thus, severe plastic deformation plus subsequent magnetic annealing offers a promising approach to the fabrication of bulk anisotropic nanostructured magnets. Further work on this issue is underway.

ACKNOWLEDGMENT

This work was supported by DARPA under Grant No. DAAD19-03-1-0038. One of the authors (B. Z. Cui) thanks the assistance of F. Ingwiller (Grenoble, France) in the sample preparation.

- ¹O. A. Ivanov, L. V. Solina, V. A. Demishima, and L. M. Magat, *Phys. Met. Metallogr.* **35**, 81 (1973).
- ²R. Skomski and J. M. D. Coey, *Phys. Rev. B* **48**, 15812 (1993).
- ³R. F. Sabiryanov and S. S. Jaswal, *J. Magn. Magn. Mater.* **177-181**, 989 (1998).
- ⁴T. Schrefl, J. Fidler, and H. Kronmüller, *Phys. Rev. B* **49**, 6100 (1994).
- ⁵T. C. Lowe and R. Z. Valiev, *Investigations and Applications of Severe Plastic Deformation* (Kluwer Academic, the Netherlands, 2000).
- ⁶N. H. Hai, N. M. Dempsey, M. Veron, M. Verdier, and D. Givord, *J. Magn. Magn. Mater.* **257**, L139 (2003).
- ⁷N. H. Hai, N. M. Dempsey, and D. Givord, *J. Magn. Magn. Mater.* **262**, 353 (2003).
- ⁸D. Li, H. Garmestani, S. R. Kalidindi, and R. Alamo, *Polymer* **42**, 4903 (2001).
- ⁹M. Verdier, M. Veron, F. Bley, F. Ingwiller, N. M. Dempsey, and D. Givord, *Philos. Mag.* **85**, 3157 (2005).
- ¹⁰K. Han, K. Yu-Zhang, H. Kung, J. D. Embury, B. J. Daniels, and B. M. Clemens, *Philos. Mag. A* **82**, 1633 (2002).
- ¹¹PCPDFWIN version 2.02, copyright © 1999 by JCPDS-ICDD.
- ¹²T. Klemmer, D. Hoydick, H. Okumura, B. Zhang, and W. A. Soffa, *Scr. Metall. Mater.* **33**, 1793 (1995).
- ¹³P. Courtois, R. P. de la Bâthie, and R. Tournier, *J. Magn. Magn. Mater.* **153**, 224 (1996).
- ¹⁴B. Z. Cui, K. Han, H. Garmestani, and H. J. Schneider-Muntau, *J. Appl. Phys.* **99**, 08E910 (2006).
- ¹⁵B. Z. Cui, K. Han, H. Garmestani, J. H. Su, H. Schneider-Muntau, and J. P. Liu, *Acta Mater.* **53**, 4155 (2005).
- ¹⁶X. J. Hao, H. Ohtsuka, and H. Wada, *Proceedings of the International Workshop on Materials Analysis and Processing in Magnetic Fields* (World Scientific, Singapore, 2005), p. 41.
- ¹⁷B. Z. Cui, C. T. Yu, K. Han, J. P. Liu, H. Garmestani, M. J. Pechan, and H. J. Schneider-Muntau, *J. Appl. Phys.* **97**, 10F308 (2005).